Materials Science and Engineering C 68 (2016) 642–650

Contents lists available at ScienceDirect

Materials Science and Engineering C

journal homepage: www.elsevier.com/locate/msec

Physicochemical properties of peptide-coated microelectrode arrays and their *in vitro* effects on neuroblast cells

Bahareh Ghane-Motlagh [a,*], Taraneh Javanbakht [b], Fatemeh Shoghi [b], Kevin J. Wilkinson [b], Richard Martel [b], Mohamad Sawan [a]

[a] Polystim Neurotechnologies Laboratory, Department of Electrical Engineering, Polytechnique Montreal, QC H3C 3A7, Canada
[b] Department of Chemistry, University of Montreal, QC H3C 3J7, Canada

ARTICLE INFO

Article history:
Received 6 August 2015
Received in revised form 25 May 2016
Accepted 13 June 2016
Available online 15 June 2016

Keywords:
Neural microelectrode array
Peptide
PEG
Hydrogel
FTIR

ABSTRACT

Silicon micromachined neural electrode arrays, which act as an interface between bioelectronic devices and neural tissues, play an important role in chronic implants, *in vivo*. The biological compatibility of chronic microelectrode arrays (MEA) is an essential factor that must be taken into account in their design and fabrication. In order to improve biocompatibility of the MEAs, the surface of the electrodes was coated with polyethylene glycol (PEG) and parylene-C, which are biocompatible polymers. An *in vitro* study was performed to test the capacity of poly-D-lysine (PDL) to improve neural-cell adhesion and proliferation. Increased proliferation of the neuroblast cells on the microelectrodes was observed in the presence of the PDL. The presence of the peptide on the electrode surface was confirmed using Fourier transform infrared spectroscopy and scanning electron microscopy (SEM). The impedance of the electrodes was not changed significantly before and after PDL deposition. Mouse neuroblast cells were seeded and cultured on the PDL coated and uncoated neural MEAs with different tip-coatings such as platinum, molybdenum, gold, sputtered iridium oxide, and carbon nanotubes. The neuroblast cells grew preferentially on and around peptide coated-microelectrode tips, as compared to the uncoated microelectrodes.

1. Introduction

Neuroprosthetic devices that can record neural activities and stimulate the central nervous system (CNS), called brain-machine interfaces (BMI), offer significant potential to restore various lost neurological functions of patients with epilepsy, Parkinson's or depression [1]. A key element in function restoration is microelectrode arrays (MEAs) implanted in neural tissues. For clinical applications, MEAs, which act as an interface between neurons and bioelectronic devices, must be reliable, stable, and efficient for long-term recording and stimulation [2]. When the MEA are inserted into brain tissue, numerous foreign body responses can occur, often resulting in a lack of biocompatibility of the implants. For example, if the electrodes are implanted for long periods of time, the formation of glial scar tissue can occur, which can encapsulate and isolate the electrodes from the neurons, resulting in a loss of electrical connectivity and increased impedance [3]. To avoid this problem, it is important to improve the biocompatibility of the electrodes.

One of the strategies that can be used to minimize immune response to implanted electrodes is by coating them with bioactive molecules such as cell adhesion peptides or proteins. These peptides not only improve cell adhesion but also increase the cell proliferation [4]. For example, peptides including Arg-Gly-Asp (RGD), Ile-Lys-Val-Ala-Val (IKVAV), Lys-His-Ile-Phe-Ser-Asp-Asp-Ser-Ser-Glu (KHIFS-DDSSE), Tyr-Ile-Gly-Ser-Arg (YIGSR), Cys-Asp-Pro-Gly-YIGSR (CDPG-YIGSR), and poly-D-lysine (PDL) have been employed [5–9]. It is important to find biomolecules that facilitate neural adhesion onto the electrode devices, minimize astrogliosis and suppress chronic microglial activation. In that light, YIGSR and IKVAV polypeptide fragments [5,6] and PDL [10] are promising candidates that are likely to modify neural cell behavior. PDL is a widely used synthetic peptide for improving neural-cell adhesion, spreading and growth, especially on metallic surfaces. Due to its positive charge, it attracts (negatively charged) neurons primarily due to electrostatic interactions [10–12].

In order to facilitate cell adhesion, proteins and peptides have been attached to solid substrates such as glass, silicon, and metals using various surface modification methods including electrochemical polymerization, covalent bonding, self-assembling monolayers, electron spinning, and peptide-polymer coating [13–18]. In a recent study, Sam et al. showed that GlyHisGlyHis could be attached to a silicon surface by electrochemical methods [19]. Conducting polymers such as polypyrole and poly(3, 4-ethylenedioxythiophene) can be added to electrode surfaces, where they can easily incorporate bioactive molecules. For example, Cui et al. were able to combine YIGSR peptide

* Corresponding author.
E-mail address: bahar.ghane@gmail.com (B. Ghane-Motlagh).

http://dx.doi.org/10.1016/j.msec.2016.06.045
0928-4931/

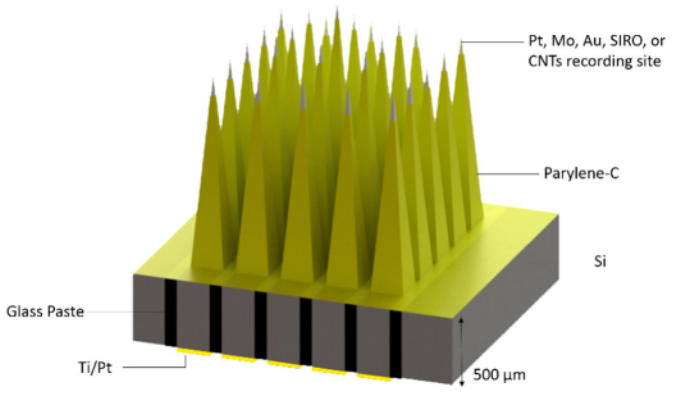

Fig. 1. Schematic view of a silicon micromachined neural MEA with variable heights of 1.45, 1.55, and 1.65 mm. The shank was covered with parylene-C (or PEG) and the recording sites of each array were coated with Pt, Mo, Au, SIRO, or CNTs. The thickness of the electrodes was 200 μm at the base and <2 μm at the tip with 100 μm spacing.

fragments from laminin onto polypyrrole coated recording sites using electrochemical polymerization [20]. The peptide-polymer coating method [14] has a number of advantages over other methods when used to cover silicon micromachined electrodes that have been coated with polymers and metals. For example, this method can be used on electrically conductive and insulating surfaces in order to cover both electrode sites and nonfunctional areas of the device. Furthermore, the peptide-polymer coating method is simpler to employ when compared with other peptide deposition methods. Among the penetrating cortical electrode arrays, silicon micromachined electrodes have a high capacity to minimize reactions with foreign bodies due to their small size and high surficial density, allowing them to record/stimulate larger volumes of neural tissue.

We have designed and fabricated novel, high-density, pyramid-shaped MEA for intracortical 3D recording and stimulation. The novel architecture of this MEA makes it unique among the currently available electrode arrays that use micromachining techniques, as it provides more contacts between the electrodes and targeted neural tissue facilitating recording from different depths of the brain. To date, penetrating silicon-based MEAs have been fabricated with two common architectures: in-plane and out-of-plane. The first architecture microelectrode contacts are patterned along the shanks. This technology provides high density of contacts; however, the shanks cause large tissue displacement and may damage significant number of neurons during insertion [21]. The second MEAs architecture—Utah and Utah Slanted electrode arrays—includes sharpened silicon needles electrically isolated from each other. The drawback of these MEAs architecture is that it is two-dimensional (2D) which provides recording data only from a plane area of the brain. Even the Slanted Utah array is quasi-3D instead of 3D [22].

In this study, the surface of the electrodes was coated with polyethylene glycol (PEG), which is a biocompatible polymer, to improve biocompatibility of the MEAs. PEG hydrogel and parylene-C are biocompatible polymers that are widely used for coating MEAs in both *in vitro* and *in vivo* studies. In order to improve neural-cell adhesion and proliferation, the surface of the electrodes was coated with PDL. An *in vitro* study was performed to test the capacity of PDL to improve neural-cell adhesion and proliferation [23–25].

The goal of this paper is to evaluate the role of PDL for promoting and stabilizing cell attachment on the surface of some unique microelectrode arrays. The impedance of the electrodes was measured before and after PDL deposition. *In vitro* cell culture tests were performed to evaluate the growth of neuroblast cells on the PDL-coated electrodes [26]. Neuroblast cells were used for the experiments due to their highest rate of spontaneous regression of all cancer types. These cells are dividing cells that will develop into neurons often after a migration phase. Because the MEAs are used to examine local responses of the neurons, we studied them with these cells.

A significant advantage of *in vitro* study is that the cell response and health can be observed over time. Optical microscopy and scanning electron microscopy (SEM) were used to evaluate the biological compatibility of the electrodes.

2. Materials and methods

2.1. Fabrication of neural MEAs

Micromachined electrode arrays were fabricated from a single block of p-type silicon (100) with a thickness of 2150 ± 25 μm and a resistivity of 0.0153–0.0158 Ω cm (University wafer, US). After micromachining, glassing, and polishing the backside, electrodes were electrically isolated [27]. The backside of the electrodes was metallized with a layer of Ti/Pt (targets with 2″ D × 2 mm thick, 99.99%, Denton

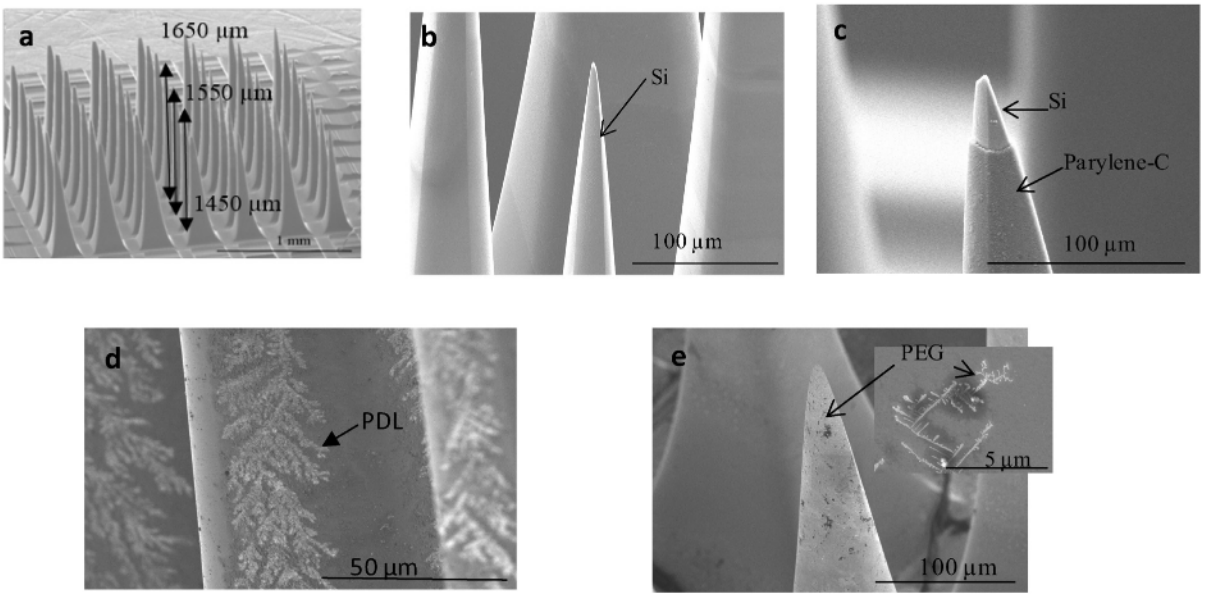

Fig. 2. SEM images of microelectrodes. (a) 3D MEAs with variable heights of 1.45, 1.45, 1.55, and 1.65 mm (the outer row was kept to protect the 5 × 5 MEA during *in vitro* test), (b) silicon-based microelectrode before coating with parylene-C and PEG, (c) microelectrode coated with parylene-C, (d) microelectrode covered with PDL, (e) microelectrode covered with PEG.

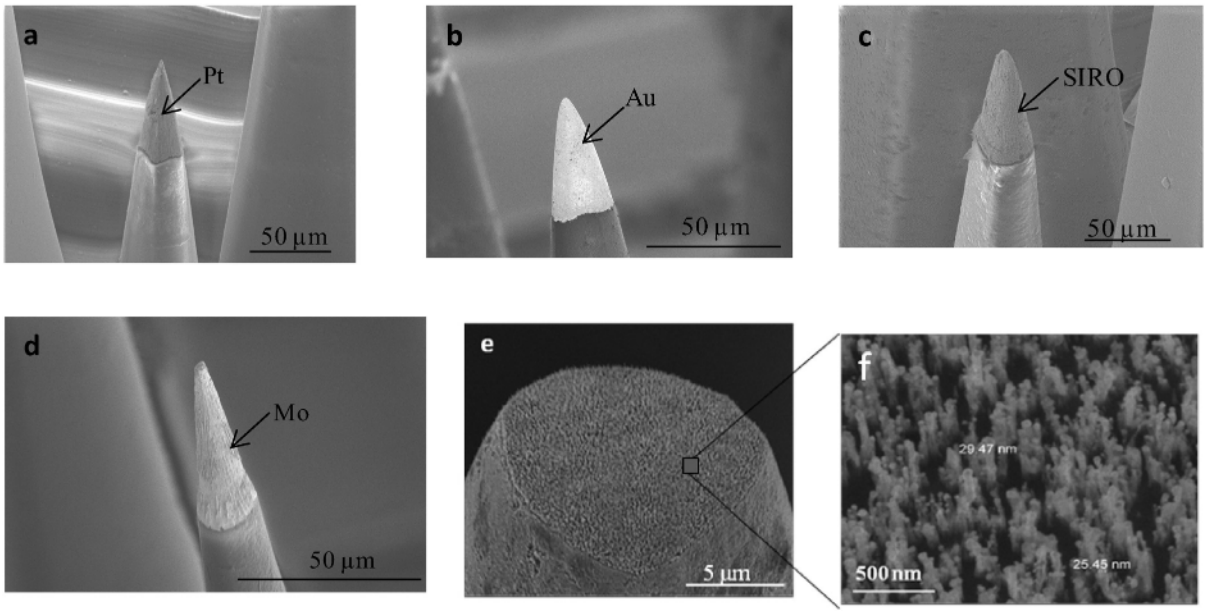

Fig. 3. SEM images of microelectrodes after metallization or CNT coating of the tips. (a) Pt, (b) Au, (c) SIRO, (d) Mo, (e & f) electrode tip coated with CNTs at different magnification.

Vacuum, US) to make electrical connection to each electrode. Pt was selected for ohmic contact, silicide formation, and wire-bonding and Ti improves the adhesion of Pt to the surface of silicon. The non-glassed side of the substrate was diced at three different depths (1.45, 1.55, and 1.65 mm), in two perpendicular directions in order to create a 5×5 matrix of rectangular columns with a spacing of 100 µm. The rectangular columns of the electrodes were converted to sharp needle shaped tips using a wet etching procedure (mixture of 49% HF and

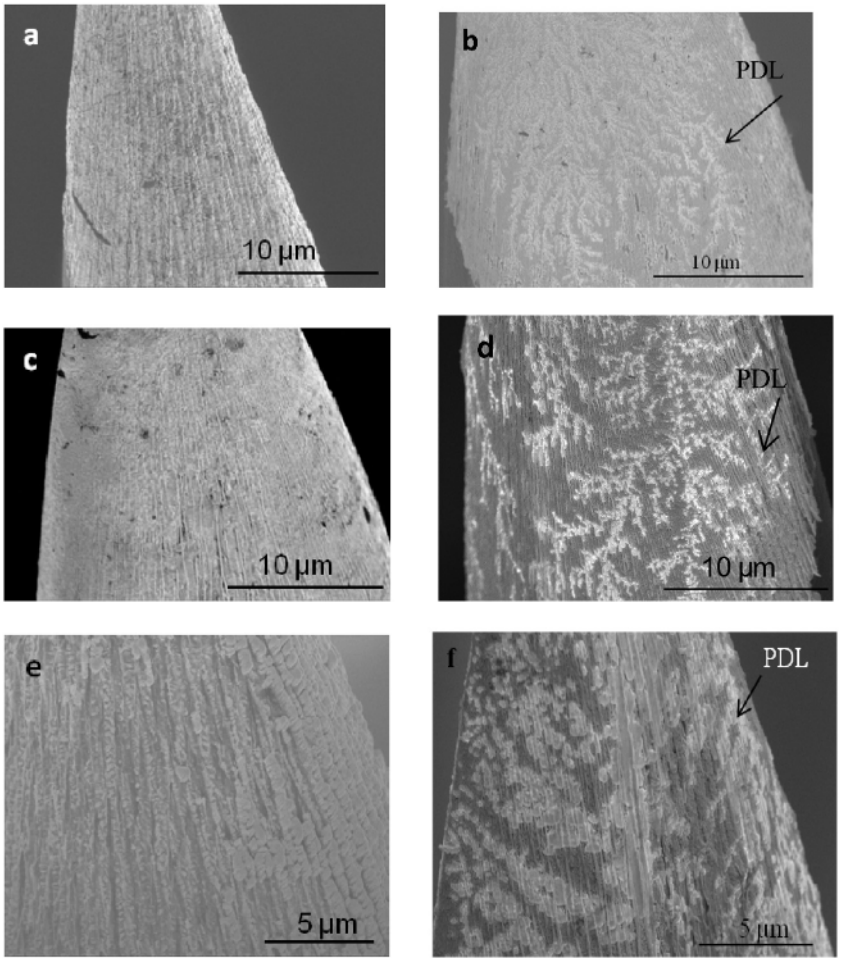

Fig. 4. SEM images of the MEA surfaces coated with, (a) and (b) Pt, (c) and (d) Au, (e) and (f) SIRO before and after coating with the PDL, respectively.

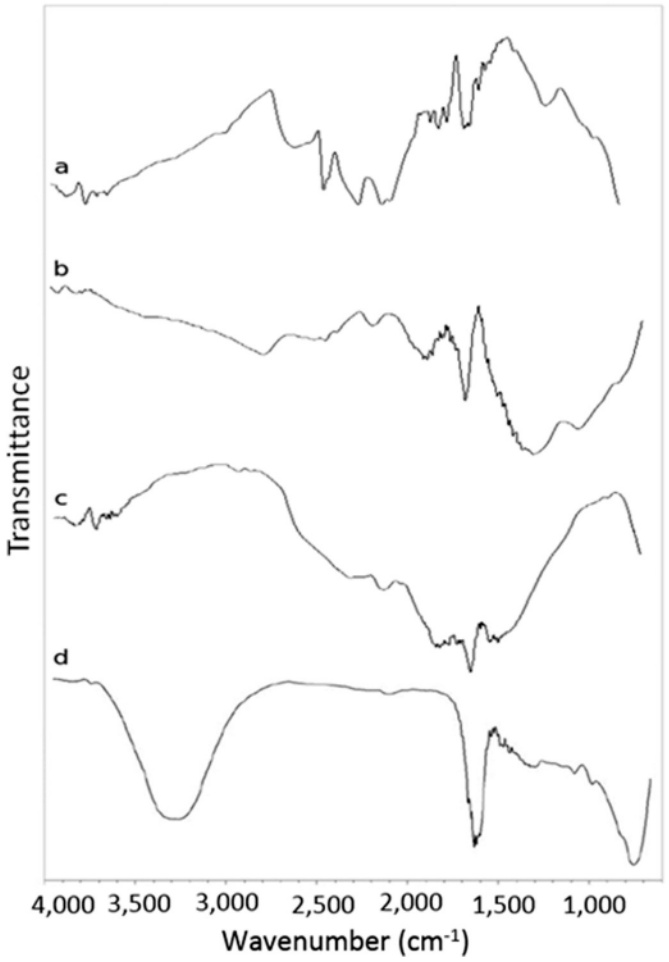

Fig. 5. FTIR spectrum of silicon MEA insulated with parylene-C and tip coated with PDL: (a) and (b) Mo tip-coating before and after coating with the PDL, respectively. (c) and (d) Pt tip-coating before and after coating with the PDL, respectively.

69% HNO_3 in a ratio of 1:19) (Fisher Scientific, US) [28,29]. Forty-five pyramid-shaped MEAs were fabricated to verify the biocompatibility of the electrodes and *in vitro* test.

SEM imaging is particularly well-suited for the characterization MEAs and is a powerful technique for assessing conducting and semiconducting materials. We used a Hitachi S-4700 field emission SEM in order to image microelectrodes and different coatings such as silicon, metals, polymers, CNTs, and peptides. The accelerating voltage for silicon and metals was 10 V and the working distance was set to ~8–10 mm. The accelerating voltage for CNTs, polymers and peptides was 1 V and the working distance was set to ~3–5 mm. The microscope has been operated in its high resolution mode and only the top secondary electron detector was enabled.

2.2. Coating of the MEAs with polymers and metals

In order to insulate the shank and improve the biocompatibility of the electrodes, the entire upper surface of some of the electrodes (*i.e.* excluding the backside) was covered with parylene-C (Cookson Electronics SCS, Italy) using a chemical vapor deposition (CVD) process. Parylene-C films were deposited using specialty coating systems (SCS, US) equipment. Parylene-C dimer was vaporized under vacuum (<10 mTorr) at 140 °C. The dimerized gas was pyrolyzed at 670 °C and deposited as a conformal, pinhole-free transparent film. The PEG (Sigma-Aldrich, CA) coating was added to the MEA by incubating them for 24 h (4 °C) in a solution of 10 mg/mL PEG in phosphate-buffered saline (PBS) at pH = 7.2 (Sigma-Aldrich, CA) [23,30]. Thirty-six arrays were coated with parylene-C whereas 3 MEAs were covered with the PEG hydrogel. Six uncoated samples were used as controls.

A novel masking technology was developed to coat the active sites of the 3D MEAs. Following insulation of the electrodes, a layer of dry-film photoresist (DuPont, FX900) was used as a mask on the array. The dry-film follows the 3D structure and enhances the uniform tip exposure [31]. Dry-film and parylene-C were removed from the tips using reactive ion etching techniques (RIE). Custom designed RIE machine was used to etch the films. In the first step, dry-film and parylene-C films were anisotropically etched by oxygen plasma from the tips at a power of 200 W, a chamber pressure of 100 mTorr for 40 min. In the next step, both films were etched isotropically from the side-walls of the electrode tips at a power of 150 W and a chamber pressure of 400 mTorr for 10 min using PVA TePla-US system.

The electrode tips of the arrays were sputter-deposited with Mo, Pt, Au, and iridium oxide (6 arrays of each metal), separately to increase the corrosion resistance, and high charge transfer characteristics and to lower impedance (Targets with 2″ D × 2 mm thick, 99.99%, Denton Vacuum, US). A novel masking technique was used to coat the tips of variable-height electrodes and improved process time and cost significantly. It would take 6 h compared to 24 h by the conventional masking method. All the metals were deposited in a custom designed multi-cathode sputtering system. Ti was used as an adhesion layer for Pt, Au, and iridium oxide. The Ti layer was sputtered in Ar ambient at the chamber pressure of 10 mTorr and gas flow rate of 10 sccm (standard cubic centimeter per minute) at the power of 90 W, for 11 min. The thickness of Ti was 100 nm. Pt and Au were sputter-deposited at the tips of 12 MEAs. Pt and Au sputtering were done in a chamber pressure of 10 mTorr with Ar flow rate of 10 sccm at the power of 90 W, for 16 and 13 min, respectively. Sputtered iridium oxide (SIRO) was deposited at the tips of 6 MEAs in Ar and O_2 plasma with both gases flow rate at 25 sccm. The power was 100 W with the deposition pressure of 5 mTorr, for 33 min. Mo was sputter-deposited on the tips of 6 MEAs at the pressure of 10 mTorr with Ar flow rate of 10 sccm. The power was 200 W, for 16 min. The thickness of Pt, Au, and Mo was 400 nm and the thickness of SIRO was 200 nm. The mask was removed with the lift-off process and ultrasonically cleaned in acetone, isopropanol, and DI water.

For 6 MEAs, electrode sites were coated with carbon nanotubes (CNTs) (Raymore, CA) using direct growth and the coffee stain methods

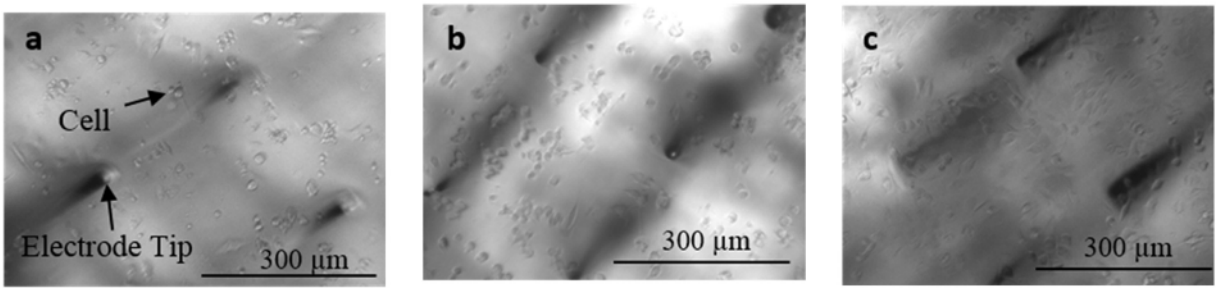

Fig. 6. Optical microscopy of the electrode tips incubated with neuroblast cells after 24 h, (a) before coating with polymers, (b) following coating with parylene-C, (c) following coating with PEG polymer.

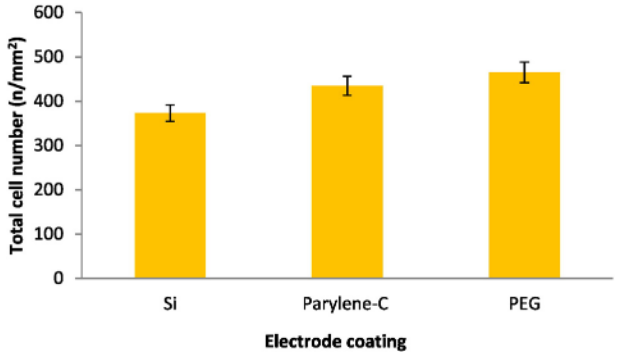

Fig. 7. Total cell number before and after parylene-C and PEG deposition, (N = 6). Cell numbers was calculated visually from the images after 24 h. In this figure 'Si' stands for non-coated tip, and'parylene-C' and 'PEG' stand for the tips after parylene-C and PEG deposition, respectively.

[32–34]. We have reported for the first time a selective direct growth of carbon nanotubes (CNTs) by using Plasma Enhanced Chemical Vapor Deposition (PECVD) on the tips of 3D MEAs. Coffee stains technique has been used as a second method for the fabrication of structurally organized single-wall carbon nanotubes (SWNTs) at the tips of the electrodes. Aqueous colloidal suspensions of sodium dodecyl sulfate (SDS) (Sigma Aldrich, CA) and SWNTs (Raymore, CA) were prepared by dispersing SDS and SWNTs in DI water through harsh sonification for 30 min. To coat electrodes with SWNTs, the MEA was dipped in a solution of SWNTs, DI water, and SDS for 24 h in a fix position. The concentrations of SDS and SWNTs were 0.2 wt.% and 3×10^{-4} wt.%, respectively. As a result, solution was drawn by capillary flow to the contact line (the electrode tip) and swept suspended particles (SWNTs) with it, which then was deposited at the tips of the electrodes. The resulting crowding particles of CNTs at the meniscus enable film formation and result in the deposition of some or all suspended particles at the edge of the droplet in the form of coffee stains. Fig. 1 shows a schematic image of the 3D MEAs. Fabrication process of MEAs has been summarized in Table S1.

2.3. Coating of peptides to the MEAs

The coating of peptides to the MEAs was carried out according to the protocol described by Smith et al. [14]. In brief, electrodes with different coatings were rinsed with acetone, isopropanol (Sigma Aldrich, US) deionized (DI) water. In the next step, MEAs were soaked in DI water for 24 h. After the cleaning process, the MEAs coated with 4×10^{-2} mg of parylene-C were immersed in solution of 0.1 mg/mL PDL (BioReagent, Sigma-Aldrich, CA) and 0.1 M phosphate buffer saline (PBS) at pH 7.4. The solutions, including electrodes, were magnetically stirred at 100 rpm for 24 h. All reactions were performed at 4 °C. Three parylene-C-coated MEAs with no metal in the tips and three arrays of each tip-coating were also covered with PDL.

2.4. Fourier transform infrared spectroscopy

Fourier transform infrared spectroscopy (FTIR) was performed in order to characterize the chemical composition of the parylene-C/PDL coatings [35,36]. A Thermo Scientific model Nicolet 6700-US spectrometer, with a SMART iTR attenuated total reflectance probe, was used to record spectra in the 500–4000 cm^{-1} range, using a 4 cm^{-1} resolution. Sixteen scans were combined in order to improve the signal-to-noise. Spectra were smoothed using Qtiplot software.

2.5. Electrical properties of the MEAs

The impedance of the electrodes was measured before and after PDL deposition using Biostat VMP-300-US system. The instrument was operated under the computer control with EC-Lab software. A solution of 0.9% PBS was used as the electrolyte [37].

2.6. Cell cultures and in vitro cell test

After deposition of the PDL, electrodes were placed in culture dishes and sterilized by ultraviolet light in a laminar flow hood. A neuroblast cell line (CCL-131), isolated from mouse muscles and obtained from American Type Culture Collection (ATCC), was used. Cells were cultured in Eagle's minimal essential medium (EMEM) (with L-Glutamine Sterile-Filtered, ATCC, US), supplemented with 10% fetal bovine serum (FBS) (ATCC, US) and 1% penicillin/streptomycin (ATCC, US) [20,38,39]. They were maintained at 37 °C in a humidified incubator with 5% CO_2 until they were seeded into convex-shaped 24-well plates. Peptide-coated and uncoated MEAs were placed separately in the middle of their own specified wells face-down with the electrode tips in contact with the well plate surface. The cell attachment and proliferation were monitored at different time spans (6, 12, 24, 48 h, and 4 days). Only one MEA was placed in each well in cell culture experiment. Every MEA was a matrix of 5×5 electrodes with 3 different heights. A Zeiss microscope (Primo Vert, US) was used to image cells on the electrode arrays after 6, 12, 24, 48 h, and 4 days. All experiments were carried out three times, using triplicate measurements.

2.7. Cell-counting

To calculate cell proliferation, the number of the cells for each convex-shaped well was determined with 2 different methods; capturing several images for each sample and manual counting of cells using hemocytometer [40].

2.7.1. Determination of cell proliferation using captured images

The amount of cells for each convex-shaped well and around each electrode tip was determined by capturing several images for each sample. The number of cells per image was counted visually with 2 persons within each circle with radius of 150 μm around each electrode tip

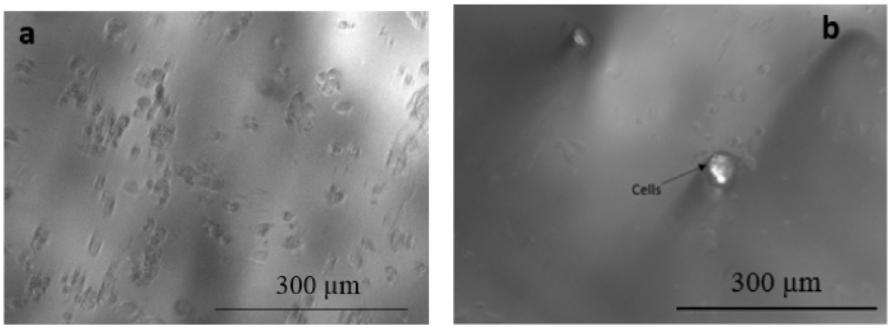

Fig. 8. Optical microscopy of (a) cell cultured media before placing MEAs. (b) The Pt-coated electrode-tip incubated with neuroblast cells after 12 h.

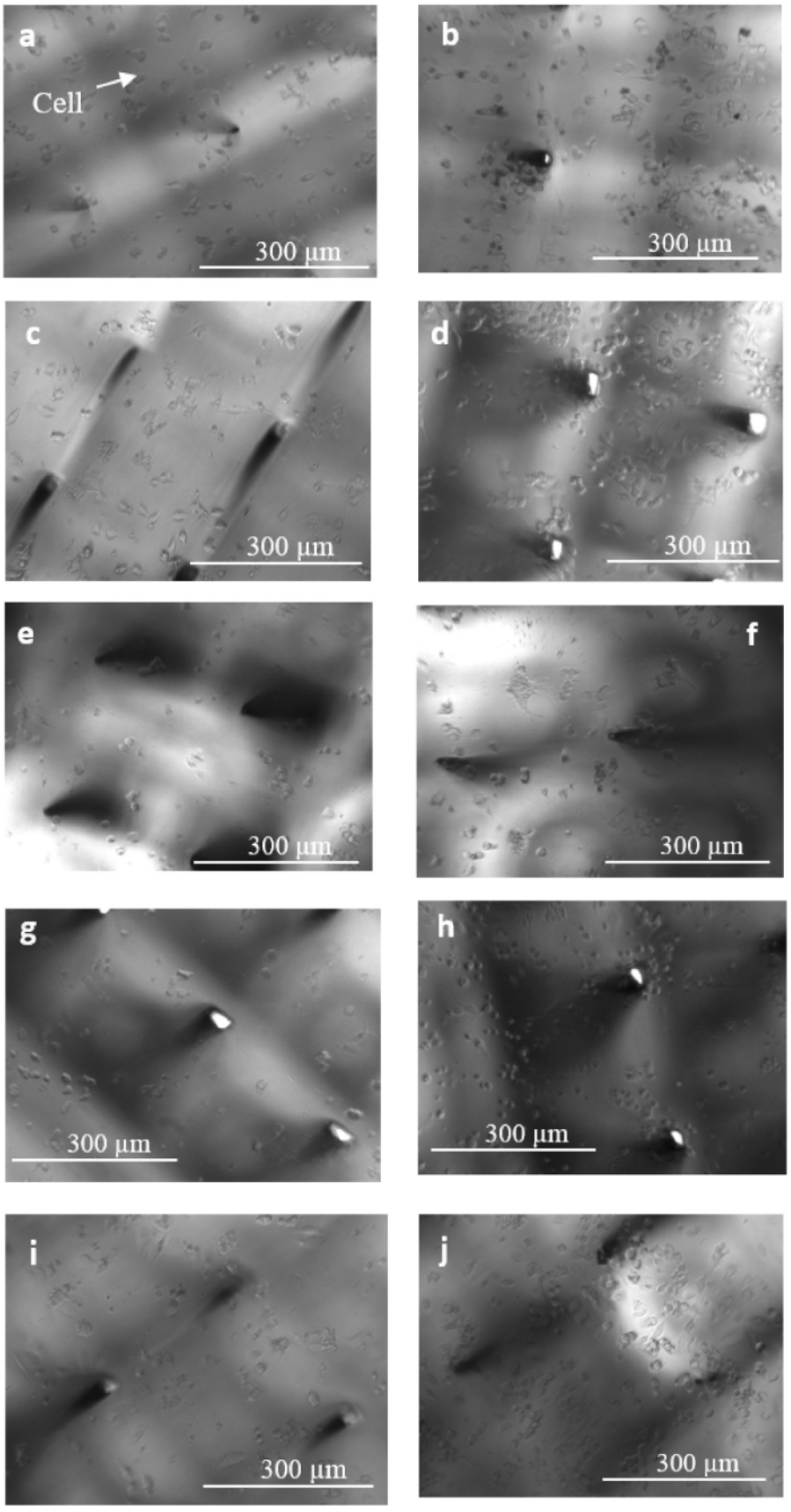

Fig. 9. Optical microscopy of the MEAs incubated with neuroblast cells. (a) and (b) Pt, (c) and (d) Au, (e) and (f) SIRO, (g) and (h) Mo, (i) and (j) CNT tips of PDL-coated and PDL-uncoated electrodes, respectively. Significantly more cells were attached to the PDL-coated electrodes than the PDL-uncoated ones.

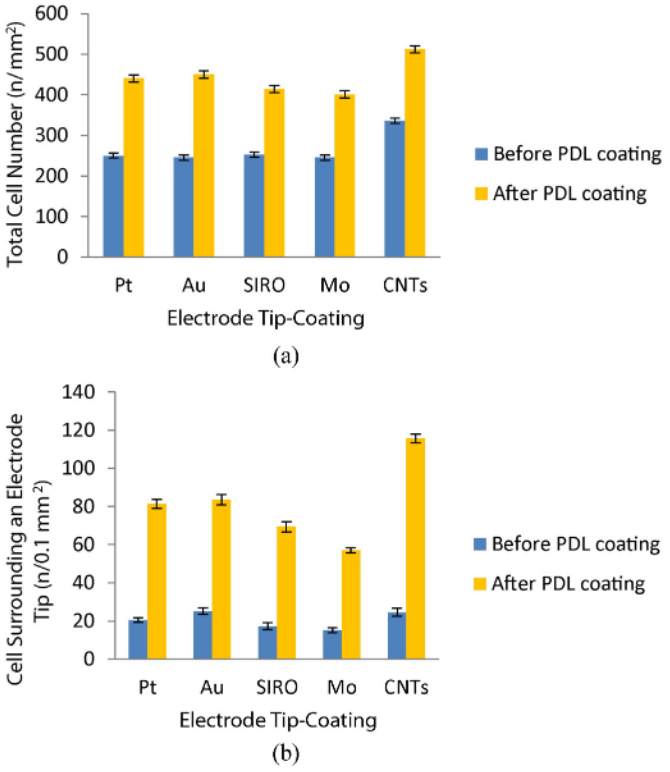

Fig. 10. Cell proliferation before and after 24 h PDL coating. (a) Total cell number of each tip-coating before and after peptide deposition. (b) Cell surrounding an electrode tip for each tip-coating before and after peptide deposition (N = 9). The cell proliferation has increased in the presence of the electrodes coated with PDL ($p = 0.0016$). Cell numbers were calculated visually from the images by two persons.

before and after PDL coating for different period of time (after 6, 12, 24, and 48 h).

2.7.2. Determination of cell proliferation manually

In this method, cells were counted manually using hemocytometer. To assure that no cells were washed away after imaging, cells were not rinsed after culture medium removal. Instead of rinsing, the cell cultures were incubated directly in trypsin. When all cells were detached, cell culture medium was added and the cells were counted.

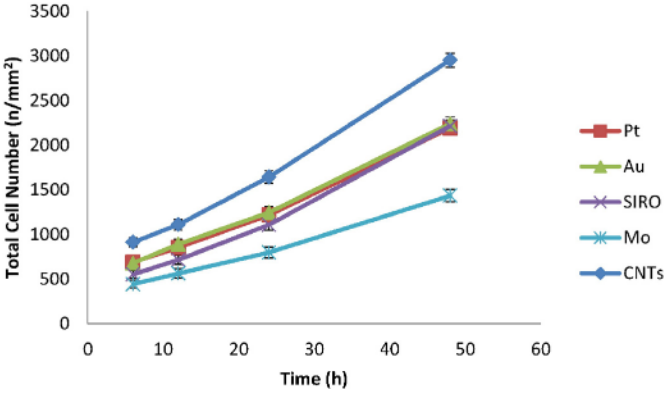

Fig. 11. Growth curve for neuroblast cells *via* manual count using hemocytometer after 6, 12, 24, and 48 h. The lines present a mean value of four points obtained in three separate experiments. Standard deviations have been indicated.

2.8. Statistical analysis

Data has been reported as the mean ± standard deviation of the mean. Cell attachment, before and after PDL deposition, was compared for statistical significance using a *t*-test (Excel) at a significance level of $p = 0.05$. Standard deviation calculations have been used. For the cell proliferation studies at least 20 images per sample were captured and counted before and after PDL coating. All experiments were repeated 3 times with triplicate samples.

3. Results

3.1. Characterization of the neural MEAs

High-density (25 electrodes/1.96 mm^2), 3D, pyramid-shaped MEAs were fabricated with variable heights of 1.45, 1.45, 1.55, and 1.65 mm (Fig. 2a). The thickness of the electrodes was 200 μm at the base and about 2 μm at the tip with 100 μm spacing (Fig. 2a). The parylene-C, PDL, and PEG coatings could be observed by SEM (Fig. 2c–e).

The active sites of each array were sputter-deposited with Mo, Pt, Au, and SIRO, separately [41]. The impedance of the electrode that the tips were coated with CNTs was decreased 5× as compared to Pt-coated electrodes. Fig. 3 shows the scanning electron micrographs of the electrode tips after parylene-C deposition and following the coating of the tips with the metals or CNTs.

3.2. Coating of peptides to MEAs

SEM images of electrode tips were acquired before and after PDL deposition followed by rinsing of the surfaces. The micrographs suggested that there was a great adhesion of the peptides onto the electrode tips. The morphology of the PDL is a nodular fractal structure that was formed finger-like patterns on the tips of the electrodes (Fig. 4).

On the other hand, no significant difference was observed for electrode impedance measured before or after coating with the PDL. The average impedance at 1 kHz of Pt, Au, SIRO, Mo, and CNT electrodes, were 70 ± 5, 120 ± 10, 4 ± 1155 ± 10, and 14 ± 2 kΩ, respectively. The CNT coating led to a 5-fold decrease in impedance compared with Pt electrode.

3.3. FTIR analysis

The attachment of PDL to the silicon MEA, insulated with parylene-C and different tip-coatings was observed by FTIR. The spectra, in the range of 600 cm^{-1} to 4000 cm^{-1}, are shown for the Pt and Mo tip-coatings before and after PDL coating (Fig. 5). CH_2 groups of lysyl residue side chains of PDL and those of parylene-C, in the range of 3200 to 2850 cm^{-1}, were masked by a broad band corresponding to the hydrogen bonding of the hydration water. The vibrational stretches of C—H at approximately 3032 cm^{-1} (again superimposed with the broad band due to hydrogen bonding), aromatic C—C stretches at 1500 cm^{-1}, aromatic C═C at 1450 cm^{-1} as well as the vibrational stretches of C—Cl at 1055 cm^{-1} could also be unambiguously attributed to the parylene-C coating of the microelectrode [35]. When PDL was added to the surfaces, N—H streching of amide groups in the range of 3100–3400 cm^{-1} and carbonyl groups in the range of 1650–1690 cm^{-1}, were also observed [36]. The coating of the PDL to the MEA with the Au, SIRO, and CNT tips was also confirmed by FTIR spectroscopy (Fig. S1).

3.4. Effect of polymer coating on the cell size, morphology, and proliferation

Cells continued to grow and proliferate when incubated with the electrodes coated with parylene-C and PEG after 4 days. The results confirmed that the electrodes and coatings were not harmful to the cells *in vitro*. When compared to the control electrodes (without coating), the

size and morphology of the cells and the cell numbers were not significantly affected by the addition of the two polymers (Figs. 6 and 7).

3.5. Cell proliferation on the peptide-coated MEAs

Peptide-coated and uncoated MEAs were cultured with mouse neuroblast cells for 4 days and monitored after 6, 12, 24, 48 h, and 4 days. Optical microscopy of cell cultured media before placing MEAs has been shown in Fig. 8a. The tips of the electrodes with different coating were in a direct contact with the cells in each well (Fig. 8b). As a result tip coating is influencing cell attachment, growth, and proliferation. In the optical images (Fig. 9), the black spots correspond to the electrode tips surrounded by the cells. An increased cell proliferation due to the PDL-coating of the samples was clearly observed by optical microscopy. Cells grew and proliferated normally in the presence of polymer, metal, and CNT coated electrodes. Indeed, the number of the cells that were quantified on the PDL-coated electrodes (five different active sites) was significantly (t-test, $p = 0.0016$) greater than the cell numbers on the uncoated electrodes (Fig. 10). The PDL coating increased cell adhesion by >50%. Fig. 11 shows growth curve for neuroblast cells *via* manual count using hemocytometer after 6, 12, 24, and 48 h. It is noteworthy that the electrodes with CNT active sites had greater cell numbers than the electrodes with metallic tips, both before and after PDL deposition. These results show that the CNTs increased biocompatibility and enhanced cellular responsiveness by attracting more neural cells, in agreement with previous work [42].

Bioactive molecules and peptides not only improve the biological compatibility of the electrodes but also can be absorbed to the CNT surface through noncovalent interactions. CNT has inherently large surface area but most of its large surface area is inaccessible in electrolyte aqueous solution and cannot contribute to charge injection and cell adhesion. Various surface modification techniques exist to enhance the hydrophilicity of the CNT electrodes. One of the techniques to modify CNTs is coating electrodes with peptides. The peptide binds strongly to the nanotube side wall *via* Van der Waals and hydrophobic interactions, while the PEG chains extend into water. As a result, the CNT-coated microelectrodes turned more hydrophilic. Another hydrophobic to hydrophilic transition happens during incubating electrodes with cell culture medium. Noncovalent binding is one of the least invasive methods to modify CNT electrodes without major disturbance of their structure. This modification can also promote cell adhesion [43]. The difference between increased cell number on Pt and Au coatings may be due to either a different molecular composition of focal contacts in cell grown on Pt/Au or different microstructural properties of the Pt/Au surfaces [44].

4. Discussion

The peptide-polymer coating method enhanced biomolecule deposition at the surface of the microelectrodes. More importantly, cells were attracted to coated electrode sites, which may improve the communication between the cells and stimulation/recording systems. Given that the experiments were performed in parallel, these results can be directly related to differences in the tip chemical compositions or the differences in the amount of PDL attached to the tips. To improve biocompatibility of the MEAs, the surface of the electrodes was covered with PEG hydrogel and parylene-C, which are biocompatible polymers. Parylene-C plays a significant role as a biocompatible polymer in implantable biomedical devices due to its unique mechanical properties and inertness. Parylene-C has a Young's modulus of ~4 GPa making it mechanically robust and highly suitable for implantable devices. In addition, parylene-C has demonstrated high stability in *in vitro* and *in vivo* studies [35,45]. PEG-based hydrogels are promising materials for working with the central nervous system because they are nonionic and relatively resistant to protein adsorption. More importantly, in culture, neuro cells that are encapsulated in PEG-based hydrogels can survive indicating that the PEG hydrogels are not cytotoxic [46]. Cells grew and proliferated in the presence of the electrodes coated with both PEG and parylene-C.

In this study, the effect of PDL on the proliferation of neuroblast cells was determined. The size and morphology of the cells were studied based on qualitative from visual appearance of optical microscopy images over 4 days. Cells were grown and proliferated normally in the presence of MEAs. Next step in this research will be functional analysis of size, morphology, and refringence of the cells. The results have shown that cells grew and proliferated normally in the presence of the electrodes and peptides. Teppola et al. optimized cell growth on MEA plates coating them with PDL, poly-L-lysine, and polyethyleneimine (PEI). Neuroblastoma cells were cultured on MEA plates before and after coating. The results showed that the MEA coating agents had a strong impact on cell morphology, growth, and viability [47]. The dynamic replacement of proteins with the bigger ones on the bio-hardware interface (including neural MEAs) results in undesired layer instabilities that are difficult to control (Vroman effect) [48,49]. Therefore, surface modification of the MEAs including polymerization and bioactive molecule-coating significantly improves the biocompatibility of neural implants in the vicinity of tissues and cells. More investigation is needed to quantify the reactive oxygen species (ROS) produced in neuroblast cells cultured with MEAs and corona proteins on the surface of these implants.

5. Conclusion

A novel, high-density, penetrating, pyramid-shaped MEA for recording and stimulation from/of neurons was designed and implemented. Due to its geometry, a high-density 3D electrode array provides more contacts between the electrodes and targeted neural tissue, which may cause more recording from different depths of the brain. Comparing this microelectrode with currently available intracortical penetrating MEAs, presented MEA has provided 3D high electrode-density (25 electrodes/1.96 mm^2) with lower impedance. The deposition of PDL on the electrodes was performed and created biologically active electrode-tissue interface. More important, PDL improved cell-adhesion and proliferation. Cells are significantly attracted to the electrode sites coated with peptides *in vitro*. After *in vitro* test, the electrodes can be implanted into the living system to act as an interface between electronics and neural tissue. Further investigation is needed to determine the biocompatibility of the MEAs on neuroblast cells. The next step will be chronic implantation of MEAs to validate long-lasting functional devices.

Acknowledgement

Authors acknowledge the financial support from NSERC and Canada Research Chairs in Smart Medical Devices. Thanks are due to May Choueib from Institut Lumière Matière, Université Claude Bernard Lyon1 and design tools and fabrication resources from CMC Microsystems.

Appendix A. Supplementary data

Supplementary data to this article can be found online at http://dx.doi.org/10.1016/j.msec.2016.06.045.

References

[1] M. Mirzaei, M. Sawan, Microelectronics-based biosensors dedicated to the detection of neurotransmitters: a review, Sensors (Basel) 14 (10) (2014) 17981–18008.
[2] J.C. Barrese, N. Rao, K. Paroo, C. Triebwasser, C. Vargas-Irwin, L. Franquemont, et al., Failure mode analysis of silicon-based intracortical microelectrode arrays in non-human primates, J. Neural Eng. 10 (6) (2013 Dec) 066014.
[3] J.N. Turner, W. Shain, D.H. Szarowski, M. Andersen, S. Martins, M. Isaacson, et al., Cerebral astrocyte response to micromachined silicon implants, Exp. Neurol. 156 (1) (1999 Mar) 33–49.

[4] V.S. Polikov, P.A. Tresco, W.M. Reichert, Response of brain tissue to chronically implanted neural electrodes, J. Neurosci. Methods 148 (1) (2005 Oct 15) 1–18.
[5] X. Cui, J. Wiler, M. Dzaman, R.A. Altschuler, D.C. Martin, In vivo studies of polypyrrole/peptide coated neural probes, Biomaterials 24 (5) (2003 Feb) 777–787.
[6] L. Kam, W. Shain, J.N. Turner, R. Bizios, Selective adhesion of astrocytes to surfaces modified with immobilized peptides, Biomaterials 23 (2) (2002 Jan) 511–515.
[7] M. Borkenhagen, J.F. Clemence, H. Sigrist, P. Aebischer, Three-dimensional extracellular matrix engineering in the nervous system, J. Biomed. Mater. Res. 40 (3) (1998 Jun 5) 392–400.
[8] M. Nomizu, B.S. Weeks, C.A. Weston, W.H. Kim, H.K. Kleinman, Y. Yamada, Structure-activity study of a laminin alpha 1 chain active peptide segment Ile–Lys–Val–Ala–Val (IKVAV), FEBS Lett. 365 (2–3) (1995 May 29) 227–231.
[9] D.S. Grant, K. Tashiro, B. Segui-Real, Y. Yamada, G.R. Martin, H.K. Kleinman, Two different laminin domains mediate the differentiation of human endothelial cells into capillary-like structures in vitro, Cell 58 (5) (1989 Sep 8) 933–943.
[10] M.J. Ignatius, N. Sawhney, A. Gupta, B.M. Thibadeau, O.R. Monteiro, I.G. Brown, Bioactive surface coatings for nanoscale instruments: effects on CNS neurons, J. Biomed. Mater. Res. 40 (2) (1998 May) 264–274.
[11] E.M. Harnett, J. Alderman, T. Wood, The surface energy of various biomaterials coated with adhesion molecules used in cell culture, Colloids Surf. B: Biointerfaces 55 (1) (2007 Mar 15) 90–97.
[12] C.D. James, R. Davis, M. Meyer, A. Turner, S. Turner, G. Withers, et al., Aligned microcontact printing of micrometer-scale poly-L-lysine structures for controlled growth of cultured neurons on planar microelectrode arrays, IEEE Trans. Biomed. Eng. 47 (1) (2000 Jan) 17–21.
[13] N.K. Guimard, N. Gomez, C.E. Schmidt, Conducting polymers in biomedical engineering, Prog. Polym. Sci. 32 (8–9) (2007 Aug-Sep) 876–921.
[14] E. Smith, J. Bai, C. Oxenford, J. Yang, R. Somayaji, H. Uludag, Conjugation of arginine–glycine–aspartic acid peptides to thermoreversible N-isopropylacrylamide polymers, J. Polym. Sci. Polym. Chem. 41 (24) (2003 Dec 15) 3989–4000.
[15] T. Pakalns, K.L. Haverstick, G.B. Fields, J.B. McCarthy, D.L. Mooradian, M. Tirrell, Cellular recognition of synthetic peptide amphiphiles in self-assembled monolayer films, Biomaterials 20 (23–24) (1999 Dec) 2265–2279.
[16] M. Huber, P. Heiduschka, S. Kienle, C. Pavlidis, J. Mack, T. Walk, et al., Modification of glassy carbon surfaces with synthetic laminin-derived peptides for nerve cell attachment and neurite growth, J. Biomed. Mater. Res. 41 (2) (1998 Aug) 278–288.
[17] M.S. Boeckl, T. Baas, A. Fujita, K.O. Hwang, A.L. Bramblett, B.D. Ratner, et al., Template-assisted nano-patterning of solid surfaces, Biopolymers 47 (2) (1998) 185–193.
[18] S.P. Massia, S.S. Rao, J.A. Hubbell, Covalently immobilized laminin peptide Tyr–Ile–Gly–Ser–Arg (YIGSR) supports cell spreading and co-localization of the 67-kilodalton laminin receptor with alpha-actinin and vinculin, J. Biol. Chem. 268 (11) (1993 Apr 15) 8053–8059.
[19] S. Sam, A.C. Gouget-Laemmel, J.N. Chazalviel, F. Ozanam, N. Gabouze, GlyHisGlyHis immobilization on silicon surface for copper detection, Appl. Surf. Sci. 269 (2013 Mar 15) 166–170.
[20] X. Cui, V.A. Lee, Y. Raphael, J.A. Wiler, J.F. Hetke, D.J. Anderson, et al., Surface modification of neural recording electrodes with conducting polymer/biomolecule blends, J. Biomed. Mater. Res. 56 (2) (2001 Aug) 261–272.
[21] K.D. Wise, Silicon microsystems for neuroscience and neural prostheses, IEEE Eng. Med. Biol. Mag. 24 (5) (2005 Sep–Oct) 22–29.
[22] R.A. Normann, Technology insight: future neuroprosthetic therapies for disorders of the nervous system, Nat. Clin. Pract. Neurol. 3 (8) (2007) 444–452.
[23] J.M. Hsu, L. Rieth, R.A. Normann, P. Tathireddy, F. Solzbacher, Encapsulation of an integrated neural interface device with parylene C, IEEE Trans. Biomed. Eng. 56 (1) (2009 Jan) 23–29.
[24] X.W. Tan, L. Hartman, K.P. Tan, R. Poh, D. Myung, L.L. Zheng, et al., In vivo biocompatibility of two PEG/PAA interpenetrating polymer networks as corneal inlays following deep stromal pocket implantation, J. Mater. Sci. Mater. Med. 24 (4) (2013 Apr) 967–977.
[25] S. Uppal, M.D. Graaf, K.D. Moeller, Microelectrode arrays and the use of PEG-functionalized diblock copolymer coatings, Biosensors 4 (2014) 318–328.
[26] E. Flampouri, S. Kintzios, Nafion and polylysine treated PEDOT mammalian cell biosensor, Procedia Eng. 25 (2011) 976–979.
[27] K.E. Jones, P.K. Campbell, R.A. Normann, A glass/silicon composite intracortical electrode array, Ann. Biomed. Eng. 20 (4) (1992) 423–437.
[28] R. Bhandari, S. Negi, L. Rieth, F. Solzbacher, A wafer-scale etching technique for high aspect ratio implantable MEMS structures, Sensors Actuators A Phys. 162 (1) (2010 Jul 1) 130–136.
[29] D.L. Klein, D.J. D'Stefan, Controlled etching of silicon in the HF-HN03 system, J. Electrochem. Soc. 109 (1) (1962) 37–42.
[30] S. Zalipsky, J.M. Harris, Introduction to chemistry and biological applications of poly(ethylene glycol), Poly(Ethylene Glycol) 680 (1997) 1–13.
[31] B. Ghane-Motlagh, M. Sawan (Eds.), High-Density 3D Pyramid-Shaped Microelectrode Arrays for Brain-Machine Interface Applications Biomedical Circuits and Systems Conference (BioCAS), IEEE, Lausanne, Swiss, 2014.
[32] J.H. Han, S.H. Choi, T.Y. Lee, J.B. Yoo, C.Y. Park, T. Jung, et al., Growth characteristics of carbon nanotubes using platinum catalyst by plasma enhanced chemical vapor deposition, Diam. Relat. Mater. 12 (3–7) (2003 Mar-Jul) 878–883.
[33] H. Li, T.C. Hain, A. Muzha, F. Schoppler, T. Hertel, Dynamical contact line pinning and zipping during carbon nanotube coffee stain formation, ACS Nano 8 (6) (2014 Jun) 6417–6424.
[34] H. Zeng, D. Wang, J. Yu, A molecule-imprinted polyaniline membrane modified on carbon fiber for detection of glycine, Biomed. Mater. Eng. 24 (1) (2014) 1085–1091.
[35] Y. Li, L. Su, C. Shou, C. Yu, J. Deng, Y. Fang, Surface-enhanced molecular spectroscopy (SEMS) based on perfect-absorber metamaterials in the mid-infrared, Sci. Rep. 3 (2013 Oct) 28–36.
[36] L. Vidal, V. Thuault, A. Mangas, R. Covenas, A. Thienpont, M. Geffard, Lauryl-poly-L-lysine: a new antimicrobial agent? J. Amino Acids 2014 (2014 Feb) 67–77.
[37] D.H. Kim, J.A. Wiler, D.J. Anderson, D.R. Kipke, D.C. Martin, Conducting polymers on hydrogel-coated neural electrode provide sensitive neural recordings in auditory cortex, Acta Biomater. 6 (1) (2010 Jan) 57–62.
[38] O. Sanchez-Ferras, B. Coutaud, T. Djavanbakht Samani, I. Tremblay, O. Souchkova, N. Pilon, Caudal-related homeobox (Cdx) protein-dependent integration of canonical Wnt signaling on paired-box 3 (Pax3) neural crest enhancer, JBC 287 (20) (2012 May) 16623–16635.
[39] O. Windl, H. Lorenz, C. Behrens, A. Romer, H.A. Kretzschmar, Construction and Characterization of Murine Neuroblastoma Cell Clones Allowing Inducible and High Expression of the Prion Protein, 801999 15–21.
[40] A. Mölder, M. Sebesta, M. Gustafsson, L. Gisselson, A.G. Wingren, K. Alm, Non-Invasive, Label-Free Cell Counting and Quantitative Analysis of Adherent Cells Using Digital Holography, 232(2)2008 Apr 240–247.
[41] P. Salvo, O.Y. Henry, K. Dhaenens, J.L. Acero Sanchez, A. Gielen, B. Werne Solnestam, et al., Fabrication and functionalization of PCB gold electrodes suitable for DNA-based electrochemical sensing, Biomed. Mater. Eng. 24 (4) (2014) 1705–1714.
[42] C. Cha, S.R. Shin, N. Annabi, M.R. Dokmeci, A. Khademhosseini, Carbon-based nanomaterials: multifunctional materials for biomedical engineering, ACS Nano 7 (4) (2013 Apr) 2891–2897.
[43] K. Wang, H.A. Fishman, H. Dai, J.S. Harris, Neural stimulation with a carbon nanotube microelectrode array, Nano Lett. 6 (9) (2006 Aug) 2043–2048.
[44] N. Turner, M. Armitage, R. Butler, G. Ireland, An in vitro model to evaluate cell adhesion to metals used in implantation shows significant differences between palladium and gold or platinum, Cell Biol. Int. 28 (28) (2004 Apr) 541–547.
[45] T.Y. Chang, V.G. Yadav, S. De Leo, A. Mohedas, B. Rajalingam, C.L. Chen, et al., Cell and protein compatibility of parylene-C surfaces, Langmuir 23 (23) (2007 Nov) 11718–11725.
[46] K.B. Bjugstad, K. Lampe, D.S. Kern, M. Mahoney, Biocompatibility of poly(ethylene glycol)-based hydrogels in the brain: an analysis of the glial response across space and time, J. Biomed. Mater. Res. A 95 (1) (2010 Oct) 79–91.
[47] H. Teppola, J. Selinummi, J.R. Sarkanen, A. Pettinen, Jalonen TO, O. Yli-Harja, et al., Automated Image Analysis of Neuroblastoma Cell Networks Cultured on Microelectrode Array Plates, Front Neuroinform Conference, Stockholm, Sweden, 2008.
[48] A. Blau, Cell adhesion promotion strategies for signal transduction enhancement in microelectrode array in vitro electrophysiology: an introductory overview and critical discussion, Curr. Opin. Colloid Interface 18 (5) (2013 Oct) 481–492.
[49] S.L. Hirsh, D.R. McKenzie, N.J. Nosworthy, J.A. Denman, O.U. Sezerman, M.M. Bilek, The Vroman effect: competitive protein exchange with dynamic multilayer protein aggregates, Colloids Surf. B: Biointerfaces 103 (2013 Mar 1) 395–404.